Orbiter–Orbiter and Orbiter–Lander Tracking Using Same-Beam Interferometry

W. M. Folkner and J. S. Border
Tracking Systems and Applications Section

Two spacecraft orbiting Mars will subtend a small angle as viewed from Earth. This angle will usually be smaller than the beam width of a single radio antenna. Thus the two spacecraft may be tracked simultaneously by a single Earth-based antenna. The same-beam interferometry (SBI) technique involves using two widely separated antennas, each observing the two spacecraft, to produce a measurement of the angular separation of the two spacecraft in the plane of the sky. The information content of SBI data is thus complementary to the line-of-sight information provided by conventional Doppler data. The inclusion of SBI data with the Doppler data in a joint orbit estimation procedure can desensitize the solution to gravity mismodeling and result in improved orbit determination accuracy. This article presents an overview of the SBI technique, a measurement error analysis, and an error covariance analysis of some examples of the application of SBI to orbit determination. For hypothetical scenarios involving the Mars Observer and the Russian Mars '94 spacecraft, orbit determination accuracy improvements of up to an order of magnitude are predicted, relative to the accuracy that can be obtained by using only Doppler data acquired separately from each spacecraft. Relative tracking between a Mars orbiter and a lander fixed on the surface of Mars is also studied. Results indicate that the lander location may be determined to a few meters, while the orbiter ephemeris may be determined with accuracy similar to the orbiter–orbiter case.

I. Introduction

Measurements of the radio signal emitted by a spacecraft orbiting another planet provide information about the spacecraft's position and velocity. A single Earth-based tracking station can directly measure line-of-sight range rate. The spacecraft trajectory can be inferred from an analysis of the time signatures imposed by the spacecraft acceleration due to gravity and by the change in geometry due to the orbital motion of the Earth and target planet. The orbit determination accuracy that can be achieved is limited by measurement system errors and errors in the spacecraft force models. The former include ground instrumental errors, clock instability, uncertain

Earth orientation, uncalibrated media delays, and errors in tracking station locations. The mismodeled forces include uncertainties in the gravity field of the central body, the force due to solar pressure, and atmospheric drag. For a low orbiter, with a period of a few hours, the uncertainties in the gravity field often dominate the orbit determination uncertainty.

Differential measurements are affected less by ground system and media errors, and desensitize orbit solutions to spacecraft force modeling errors. Differential measurements studied for low orbiters such as Magellan or Mars Observer (MO) include differenced-Doppler and delta differential one-way Doppler (ΔDOD). Differenced-Doppler involves the use of two tracking stations to measure the Doppler shift of the spacecraft carrier, with one of the stations providing a stable uplink frequency. A clock rate offset between the two stations introduces a systematic error into this measurement. The ΔDOD measurement subtracts the differential spacecraft Doppler from the differential frequency shift of a quasar to calibrate the station clock offset. Both of these measurement types give, essentially, a measurement of the spacecraft velocity in the plane of the sky (the plane perpendicular to the Earth–spacecraft line of sight). This type of measurement has been shown to improve orbit determination accuracy in case studies for Magellan [1].

For a number of upcoming interplanetary missions, primarily directed towards Mars, two spacecraft may simultaneously be in orbit about the same planet. This opens the possibility of differential measurements between the two spacecraft instead of between a spacecraft and a quasar. The angle between the two spacecraft as viewed from Earth will be much smaller than the usual spacecraft–quasar angle, which is typically 10 deg. Since many measurement errors scale with the angular separation, the spacecraft–spacecraft measurement is potentially much more accurate than conventional interferometric measurements. If the two spacecraft lie within the beam width of a single antenna, as will often be the case, the carrier phases of both spacecraft can be simultaneously tracked. This use of phase rather than group delay (or delay rate) further increases the measurement accuracy. It is predicted that the same-beam interferometry (SBI) measurement accuracy could be up to three orders of magnitude better than that for conventional spacecraft–quasar interferometry [2,3].

The utility of SBI measurements will depend on a number of factors, such as the data arc length, data accuracy and weighting, orbital geometry, and gravity modeling uncertainties. The analysis presented here is not meant to be definitive but rather to show the relative power of adding SBI data to nominal Doppler tracking strategies. The sample cases presented below are based on the Russian Mars '94 mission arriving at Mars while MO is nearing the end of its prime mission. An earlier opportunity to perform SBI measurements and demonstrate their utility for orbit determination occurred in August 1991 when Magellan joined Pioneer 12 in orbit about Venus [4].

A more futuristic case involves relative tracking with respect to landers on the surface of Mars. There are many possible applications which then arise, including lander–rover tracking for rover position estimation, or lander–spacecraft tracking for spacecraft approaching the planet. The potential use of SBI to determine relative lander–rover positions at the meter level has been discussed briefly elsewhere [5]. The only case involving a lander included below involves the use of SBI for tracking an orbiting spacecraft with respect to a lander.

II. Same-Beam Interferometry Technique

The SBI measurement of two spacecraft is depicted in Fig. 1. Two ground stations measure the phase of the carrier signal from each spacecraft as a function of time. The measured phase, when differenced between spacecraft and differenced between ground stations, gives an instantaneous measurement of the separation of the two spacecraft in the plane of the sky (in the direction along the projected baseline). The relative measurements can be included in a joint orbit estimation process along with Doppler data obtained from each of the two spacecraft. The use of all the data in a single estimation process ties both orbits to the center of gravitation through the dynamic signatures in the data.

The SBI measurement is similar to a delta differential one-way range (ΔDOR) measurement [6] in that an observable is formed from the observation of two sources at two widely separated ground stations. The ΔDOR measurement determines the spacecraft differential one-way range and compares this with the interferometric delay of an angularly nearby quasar to calibrate the ground station clocks and other common mode errors. The ΔDOR measurement uses tones modulated on the downlink carrier to determine the group delay, with a precision of a fraction of the wavelength corresponding to the spanned bandwidth. This wavelength is about 7.5 m for the 40-MHz spanned bandwidth for X-band (8.4-GHz) ΔDOR measurements. The SBI measurement has the advantage of a much smaller angular separation between the two spacecraft in orbit (a fraction of a milliradian) than the

spacecraft–quasar separation for a ΔDOR measurement (typically 10 deg or about 175 mrad). The SBI measurements determine the phase delay to a precision of a fraction of the carrier wavelength, which is 3.6 cm at X-band. The combination of smaller angular separation and the use of phase delay rather than group delay results in a theoretical accuracy for SBI measurements of 0.2 mm compared with the 14-cm accuracy of conventional X-band ΔDOR measurements.

SBI has some operational advantages over conventional spacecraft interferometry. Since no quasar is used, there is no need to change the pointing of the antennas away from the spacecraft. Without the quasar, there is also no need for a cross-correlation step in the data processing. Appropriately designed receivers could simultaneously extract the phase measurements in real time. The phase measurements would then be processed much like conventional Doppler data.

The SBI data do not determine the doubly differenced carrier phase unambiguously. Each arc of SBI measurements begins with a phase bias, which consists of an integer number of cycles and a possible fractional phase due to imperfectly calibrated instrumental delays. Provided that the calibration of the station instrumentation is sufficient to determine the fractional phase to a level small as compared with the SBI data noise, the phase bias can be constrained to be an integer number of cycles. The phase bias must be provided from a priori information or else a phase bias must be estimated for each SBI data arc. The phase bias could be determined from group delay measurements (using widely spaced tones about the carrier) or from a sufficiently accurate a priori orbit solution. In particular, if the orbit solution using SBI data with the phase bias estimated as a real number can determine the bias to a small fraction of a cycle, then the phase bias can be confidently fixed to the nearest integer. A subsequent orbit solution will result in greater orbit determination accuracy.

An error budget for X-band SBI measurements is presented in Table 1. The error budget assumes a Sun–Earth–Probe (SEP) angle of 20 deg, a spacecraft separation angle $\Delta\theta$ of 100 μrad, an Earth–spacecraft distance of 1.4 AU, and a projected baseline length of 8000 km (a representative value for intercontinental baselines). The largest error contribution listed is from imperfect delay cancellation due to solar plasma. Nearly all charged-particle effects could be removed by dual-frequency measurements. However, the upcoming opportunities for SBI measurements are not assured of having two frequencies from both spacecraft. The particular case studied below occurs when the Russian Mars '94 mission arrives at Mars in 1995 while MO is still active. The Mars '94 spacecraft will have an X-band transmitter to provide a signal for ΔDOR measurements to be acquired by the DSN during cruise, but it will rely on C-band (6-GHz) transmissions for telemetry and conventional Doppler and range tracking. MO will use X-band for telemetry and navigation although it does have an experimental 34-GHz capability. Often the charged-particle effects will be less than those shown in Table 1 since the solar plasma effects will be less at SEP angles larger than 20 deg. In that respect the measurement error budget given in Table 1 is somewhat conservative. The terms in the error budget are briefly discussed below.

A. Solar Plasma

The solar plasma error has been calculated by using a thin-screen frozen turbulence model [7]. The differential delay error is computed numerically; sample results are shown in Fig. 2. It can be seen that for these small spacecraft separation angles, the differential delay error is approximately linear with separation angle and SEP angle. The applicability of this model to SBI measurements will need to be tested by taking some experimental data.

B. Ionosphere

Ionosphere calibration is provided to the DSN from Global Positioning System (GPS) measurements. The error in the Earth's ionospheric delay mapped to any line of sight after calibration is approximately 30 mm at X-band [8]. The differential delay error ε_d for two nearby lines of sight is taken to be

$$\varepsilon_d \text{ (mm)} = 30 \text{ mm} \times \Delta\theta \times F \times \sqrt{2} \qquad (1)$$

where $\Delta\theta$ is the spacecraft separation angle (in radians), F is a factor representing the derivative of the mapping function with respect to angle in the direction of $\Delta\theta$, and the $\sqrt{2}$ factor is introduced because there are independent errors at each station. The mapping functions represent the largest uncertainty in ionospheric calibrations and are not well known for the small separations needed for SBI data. The derivative of the mapping function used for GPS calibrations has a maximum value of 3.5/rad if the separation angle occurs in elevation. Here a value of 5/rad for the derivative of the mapping function was assumed to be somewhat more conservative. More study will be needed to better understand the ionospheric error for SBI.

C. Troposphere

The tropospheric error is represented by

$$\varepsilon_d \text{ (mm)} = \sqrt{2} \times \Delta\theta \times 40 \text{ mm} \times \cos(E)/\sin^2(E) \qquad (2)$$

where E is the elevation angle, $\Delta\theta$ is the difference in elevation angle between the two spacecraft, and the troposphere delay error is taken to be a zenith value of 40 mm mapped to lower elevations as $(1/\sin(E))$. For the troposphere error listed in Table 1, an elevation value of 15 deg and an elevation difference of 100 μrad is assumed for the two spacecraft. A factor of $\sqrt{2}$ accounts for the separate errors at two ground stations.

D. System Noise

The received signal contains the spacecraft signals and ground-receiver generated noise, which is proportional to the system operating temperature. The system noise error depends on the ratio of received signal power to noise power. The voltage signal-to-noise ratio (SNR_v) can be made higher by averaging over a longer time interval. The SBI phase error due to system noise is given by

$$\varepsilon_d \text{ (mm)} = \lambda\sqrt{2}/(2\pi SNR_v) \tag{3}$$

where λ is the X-band wavelength (36 mm). With nominal Mars '94 transmitter power of 1 W and antenna gain of 17 dB at X-band, a DSN 34-m antenna achieves an SNR_v value of 175 for an integration time of 5 min. The MO SNR_v will be approximately 10 times higher due to the greater effective transmitted carrier power. There is a separate error for Mars '94 (neglecting the MO SNR_v error) at each station, which results in the factor of $\sqrt{2}$.

E. Phase Dispersion

The SBI observable is generated by double differencing the measured phase of sinusoidal signals transmitted from two spacecraft and received at two stations. The ground receiver chains introduce phase shifts which depend on the Doppler shifted signal frequencies, and hence will in general be distinct for each station and for each spacecraft. Instrumental phase shifts can be divided into two categories: phase shifts which vary linearly with frequency (nondispersive) and phase shifts which have a nonlinear frequency dependence (dispersive). Nondispersive instrumental errors are estimated below in Subsection II. Dispersive errors are approximated by

$$\varepsilon_d \text{ (mm)} = 2 \times (0.5 \text{ deg}) \times \lambda/(360/\text{deg}) \tag{4}$$

where 0.5 deg is representative of the instrumental phase dispersion in the operational VLBI receiver system [9]. A separate error occurs for each spacecraft at each ground station leading to the factor of 2. The phase dispersion effects can be reduced by better instrumentation or very close spacecraft frequencies.

F. Oscillator Drift

An unknown offset between the transmitter frequencies of the two spacecraft will cause an error given by

$$\varepsilon_d \text{ (mm)} = c\tau \times \Delta f/f \tag{5}$$

where c is the speed of light, τ is the difference in reception time at the two stations (here assumed to be 10 msec), f is the nominal transmitter frequency for each spacecraft, and Δf is the unknown transmitter frequency offset. For two-way transmissions, where separate uplinks derived from independent frequency standards are used for the two spacecraft, an estimate of $\Delta f/f$ is provided by the expected accuracy of the station clock rate calibration, which is 5×10^{-14}. For one-way transmissions, line-of-sight Doppler measurements are used to estimate corrections to the nominal spacecraft onboard oscillator frequency. The accuracy to which the oscillator frequency can be estimated depends on the tracking coverage and on the oscillator stability; $\Delta f/f$ can typically be estimated with an accuracy of 2×10^{-12} for one-way transmissions.

G. Baseline

Since an angular measurement is derived from knowledge of the time of reception at two Earth ground stations, uncertainty in station location and Earth orientation degrades the interpretation of the SBI measurement. The Earth's pole orientation and rotation rate change randomly and must be monitored to maintain knowledge of these quantities. Currently at JPL, knowledge of the Earth's orientation is being maintained with an accuracy of 30 cm for real-time data analysis. For analysis of data more than two weeks old, the error in Earth orientation is less than 5 cm. The Earth orientation accuracy for real-time analysis could be improved if required and is expected to improve to the 5-cm level as measurements from the GPS are included in the coming years [10,11,12]. DSN station locations have been determined with an accuracy better than 5 cm by VLBI and satellite laser ranging [13,14]. Overall, the value of 7 cm is used to represent the baseline error due to station location and Earth orientation uncertainties. The SBI error is given by

$$\varepsilon_d \text{ (mm)} = 70 \text{ mm} \times \Delta\theta \tag{6}$$

H. Station Instrumentation

An uncalibrated group delay or clock offset in the ground station instrumentation causes a phase delay error of the form

$$\varepsilon_d \text{ (mm)} = (\dot{\rho}_1 - \dot{\rho}_2)\,\delta\tau_I \qquad (7)$$

where $\dot{\rho}_i$ is the line-of-sight range rate (mm/sec) between one station and spacecraft i, and $\delta\tau_I$ is the uncalibrated instrumentation delay (sec). This error varies slowly over a pass as the Doppler shift changes. The MO dynamics are used to bound this error, since Mars '94 is in a slower orbit. Over a 1-hr data arc, the range-rate change is bounded by 6×10^6 mm/sec. All station delays should be calibrated to 2×10^{-8} sec. The resulting SBI error due to nondispersive instrumental effects drifts by no more than 0.12 mm.

III. Orbiter–Orbiter Tracking Example

The Russian Mars '94 mission will nominally arrive at Mars in mid-1995 near the end of the MO primary mission. It will be possible to make SBI measurements at X-band by using Mars '94 and MO. Sample orbital elements for Mars '94 were chosen for the epoch June 1, 1995, at 19:50 UT. These, along with orbital elements for MO at the same epoch, are listed in Table 2. At this time, the Earth–Mars distance is 1.4 AU, the right ascension and declination of Mars as seen from Earth are 155.9 deg and 11.5 deg, respectively, and the SEP angle is 82.4 deg. A plot of the orbits in the plane of the sky as seen from Earth is shown in Fig. 3. The separation angle between the two spacecraft is always less than 100 μrad, so both spacecraft will lie within the X-band beamwidth of a 34-m antenna, which is 1.06 mrad.

Covariance analyses have been performed based on an early version of the MO Navigation Plan.[1] Both MO and Mars '94 were assumed to have area-to-mass ratios equal to 0.017 m^2/kg. For study purposes, a nominal 12-hr tracking arc was used, including Doppler data for both spacecraft from an antenna at the Goldstone, California, DSN complex. The data arc includes six orbits of MO and one orbit for Mars '94. The spacecraft modeling assumptions are outlined in Table 3. In each case, only the spacecraft epoch state is estimated. The dominant error in the following analyses is usually the "considered" (unadjusted) gravity field uncertainty. The gravity field uncertainty is based on an analysis of gravity calibration orbits for MO early in its mission.[1] These values will evolve as further studies are performed and as the MO mission progresses.

The following cases show orbit determination uncertainties over the 12-hr period during which Doppler data are scheduled. SBI data, when taken, also lie within this interval. This study is confined to investigating orbit determination accuracy for trajectory reconstruction purposes. Orbit determination for prediction purposes, which is of interest for mission operation, is more susceptible to force modeling assumptions and is not addressed here.

A. Doppler-Only Solutions

The orbit determination uncertainty for MO by using only Doppler data is presented in Fig. 4, which shows the rss position error during the 12-hr time interval. The Doppler data were weighted at 0.1 mm/sec for a 3-min integration time. The relatively low errors result from the multirevolution data span and the fairly low gravity field uncertainties derived from the gravity calibration orbit, which nonetheless still dominate the orbit determination uncertainty. For Mars '94, the Doppler data, spanning one orbit, were also weighted at 0.1 mm/sec for a 3-min integration time. The Doppler-only Mars '94 orbit determination uncertainty is shown in Fig. 5. The dominant error is the computed error (due to random measurement noise) rather than the considered gravity field error.

The Doppler-only orbit determination uncertainty for both MO and Mars '94 is limited by the ability of a single pass of Doppler data to determine the longitude of the ascending node in the plane of the sky. For the nearly circular MO orbit, the node uncertainty appears (in Fig. 4) as a twice-per-orbit signature. For the Mars '94 orbit, the node uncertainty shows up (in Fig. 5) as a once-per-orbit signature in the position uncertainty with maximum uncertainty at apoapsis.

B. Doppler Plus SBI

For this case, a joint orbit analysis was performed with SBI data employed in addition to Doppler data. SBI data were scheduled during the first four hours of the Doppler interval, during the mutual visibility period for Goldstone and the Madrid DSN complex, and for the last three hours of the Doppler interval, during the mutual visibility period for Goldstone and the Canberra DSN complex. The SBI data were weighted at 0.29 mm for a 5-min integration time. Phase biases were not estimated for this case since the Doppler-only results are sufficiently accurate to fix the phase biases, at least near the periapsis for Mars '94. The Doppler data were deweighted to 1 mm/sec to reduce sensitivity to gravity field errors in the estimation process. The orbit determination errors are shown in Figs. 6 and 7. The MO position uncertainty of about 10 m consists of approximately equal contributions of computed error and gravity field uncertainty. The SBI data accuracy of 0.29 mm (for 5-min integrations) equates to an effective

[1] P. B. Esposito, *Mars Observer Navigation Plan: Preliminary*, JPL D-3820 (internal document), Jet Propulsion Laboratory, Pasadena, California, December 16, 1988.

angular accuracy of about 36 prad, which corresponds to ~8 m at the 1.4-AU Earth–Mars distance. For MO, orbit determination accuracy is approaching the limit of the data accuracy. The Mars '94 position uncertainty of about 50 m is dominated by considered gravity field uncertainty.

C. One-Way Doppler Option for Mars '94

In order to track Mars '94 entirely from the DSN, one-way Doppler may have to be used instead of two-way Doppler. This is because the Mars '94 mission will not have two-way Doppler capability at X-band, instead relying on C-band Doppler from the C-band telemetry for routine navigation. Since the DSN will not support C-band, either Russian Doppler data or one-way Doppler at X-band are needed for orbit determination. The one-way Doppler case is also of interest since the DSN antennas can currently transmit only a single uplink frequency. By using one-way Doppler from the second spacecraft, telemetry and navigation for two spacecraft could be done from one antenna at each complex.

One-way Doppler accuracy will be limited by the stability of the oscillator on the Russian spacecraft. To examine the use of one-way X-band Doppler, the Mars '94 oscillator was assumed to have the characteristics shown in Fig. 8. This curve approximates the performance of the ultrastable oscillator on the Soviet Phobos spacecraft. One-way Doppler data were included with weight 0.75 mm/sec for a 3-min integration time, with a constant frequency offset and random walk in frequency modeled as estimated parameters to represent the spacecraft oscillator behavior.

Figure 9 shows the orbit determination accuracy for Mars '94 using only one-way Doppler for the 12-hr view period from Goldstone. The results are much worse than the two-way Doppler results of Fig. 5. However, the one-way Doppler, combined with MO two-way Doppler and SBI data, gives good results. Orbit determination accuracies that result from using 12 hr of two-way Doppler from MO weighted at 1 mm/sec, 12 hr of one-way Doppler from Mars '94, and SBI from both DSN baselines are shown in Figs. 10 and 11. In obtaining these results, phase biases were estimated. The MO accuracy shown in Fig. 10 is comparable to the results obtained when two-way Doppler and SBI data are used for both spacecraft. The Mars '94 results in Fig. 11 are not as good as the two-way Doppler-only solution for Mars '94 shown in Fig. 5. The orbital accuracy for these solutions is marginal in terms of being able to determine the correct phase biases for the SBI data. If the biases could be fixed (perhaps by using multiple tones), the orbit determination accuracy would be improved to the levels shown in Figs. 12 and 13.

IV. Orbiter–Lander Tracking Example

There are several potential missions which would place landers or rovers on the surface of Mars. The communications capability of the landers is not yet known. But in order to examine the utility of tracking an orbiter with respect to a lander, this study arbitrarily included a lander located at Mars latitude of +26 deg and longitude of 140 deg. This lander was assumed to be able to communicate with the Earth at X-band and be capable of supporting two-way Doppler tracking from DSN stations. The lander was tracked at the same time as the MO spacecraft in the above cases. Because of the relative rotation of Earth and Mars, the lander was visible from Goldstone for only the first four hours of the data period. An orbit solution covariance was calculated with 12 hr of Doppler data for MO, weighted at 1 mm/sec, 4 hr of Doppler data from the lander weighted at 1 mm/sec, and 4 hr of SBI data from the Madrid–Goldstone baseline weighted at 0.2 mm. The SBI phase bias was presumed to be fixed. The position of the lander with respect to the center of Mars was assumed to be known a priori to 100 km and was estimated along with the spacecraft state.

The resulting orbital accuracy for MO is shown in Fig. 14 and is comparable to the orbiter–orbiter tracking results shown in Fig. 10. The estimated lander position accuracy, given in Fig. 15, is a few meters in spin radius and longitude and 20 m in height (Z) above Mars' equator. This position accuracy is good enough that random orientation changes for Mars, analogous to terrestrial polar motion and rotation rate changes, will become observable. This suggests that orbiter–lander tracking, or differential tracking between multiple landers, can be used for studies of Mars rotation in addition to navigation.

Another tracking scenario studied included one-way Doppler from the lander (with the same assumed oscillator as for the one-way Mars '94 study above) in addition to two-way Doppler from MO and SBI data. The orbit determination errors for MO were found to be comparable to those shown in Fig. 14. However, the estimated lander position uncertainty increased to 20 m in longitude and spin radius and 80 m in Z. Thus, one-way Doppler from the lander is adequate for determination of the orbiter trajectory. For accurate location of the lander, either two-way Doppler must be used or some other strategy, such as the use of a longer data arc or a more stable oscillator, must be adopted.

V. Conclusion

Same-beam interferometry data, combined with two-way Doppler or a combination of two-way and one-way

Doppler, has the potential to be a powerful orbit determination data type and allows multiple spacecraft to be tracked simultaneously. Orbit determination studies using MO and the Russian Mars '94 spacecraft have predicted accuracy improvements of an order of magnitude or more over Doppler-only orbit solutions for short data arcs. Also, it should be possible to obtain 1-km orbit determinati accuracy for Mars '94 in downlink-only mode when track with respect to MO. SBI tracking of a lander on Mars and Mars orbiter can potentially yield position accuracies f Mars landers at the few-meter level by using single-d data arcs.

Acknowledgments

The authors thank A. S. Konopliv for help with the covariance software used and R. D. Kahn for assistance with the solar plasma error model.

References

[1] S. N. Mohan and P. B. Esposito, "Venus Radar Mapper Orbit Accuracy Analysis," paper 84-1986, presented at the AIAA/AAS Astrodynamics Conference, Seattle, Washington, August 1984.

[2] J. S. Border and W. M. Folkner, "Differential Spacecraft Tracking by Interferometry," paper CNES-89-145, presented at the CNES International Symposium on Space Dynamics, Toulouse, France, November 1989.

[3] J. S. Border and R. D. Kahn, "Relative Tracking of Multiple Spacecraft by Interferometry," paper 89-178, presented at the AAS/GSFC International Symposium on Orbital Mechanics and Mission Design, Greenbelt, Maryland, April 1989.

[4] W. M. Folkner and J. S. Border, "Orbit Determination for Magellan and Pioneer 12 Using Same-Beam Interferometry," paper AAS 91-393, presented at the AAS/AIAA Astrodynamics Specialist Conference, Durango, Colorado, August 19–22, 1991.

[5] R. D. Kahn, W. M. Folkner, J. S. Border, and A. J. Vijayaraghavan, "Position Determination of a Lander and Rover at Mars With Earth-Based Differential Tracking," *TDA Progress Report 42-108*, vol. October–December 1991, Jet Propulsion Laboratory, Pasadena, California, pp. 279–293, February 15, 1992.

[6] J. S. Border, F. F. Donivan, S. G. Finley, C. E. Hildebrand, B. Moultrie, and L. J. Skjerve, "Determining Spacecraft Angular Position with Delta VLBI: The Voyager Demonstration," paper 82–1471, presented at the AIAA/AAS Astrodynamics Conference, San Diego, California, August 1982.

[7] R. D. Kahn and J. S. Border, "Precise Interferometric Tracking of Spacecraft at Low Sun–Earth–Probe Angles," paper 88-0572, presented at the AIAA 26th Aerospace Sciences Meeting, Reno, Nevada, January 1988.

[8] G. E. Lanyi and T. Roth, "A Comparison of Mapped and Measured Total Ionospheric Electron Content Using Global Positioning System and Beacon Satellite Observations," *Radio Science*, vol. 23, no. 4, pp. 483–492, July–August 1988.

[9] N. C. Ham, "VLBI System (BLK 1) IF-Video Down Conversion Design," *TDA Progress Report 42-79*, vol. July–September 1984, Jet Propulsion Laboratory, Pasadena, California, pp. 172–188, November 15, 1984.

[10] A. P. Freedman, "Measuring Earth Orientation with the Global Positioning System," *Bulletin Geodesique*, vol. 65, pp. 53–65, 1991.

[11] S. M. Lichten, S. L. Marcus, and J. O. Dickey, "Sub-Daily Resolution of Earth Rotation Variations with Global Positioning System Measurements," *Geophys. Res. Lett.* (in press).

[12] U. J. Lindqwister, A. P. Freedman, and G. Blewitt, "Daily Estimates of the Earth's Pole Position with the Global Positioning System," *Geophys. Res. Lett.* (in press).

[13] J. R. Ray, C. Ma, J. W. Ryan, T. A. Clark, R. J. Eanes, M. M. Watkins, B. E. Schutz, and B. D. Tapley, "Comparison of VLBI and SLR Geocentric Site Coordinates," *Geophys. Res. Lett.*, vol. 18, no. 2, pp. 231–234, February 1991.

[14] M. H. Finger and W. M. Folkner, "A Determination of the Radio-Planetary Frame Tie and the DSN Tracking Station Locations," paper AIAA 90-2905, presented at the AIAA/AAS Astrodynamics Conference, Portland, Oregon, August 20–22, 1990.

Table 1. X-band same-beam error budget (for 5-min integration time and 20-deg Sun–Earth–Mars angle).

Error source	Error, mcycles	Error, mm	Error, prad
Solar plasma	6.2	0.22	28
Ionosphere	0.6	0.02	3
Troposphere	2.2	0.08	10
System noise	1.3	0.05	6
Phase dispersion	2.8	0.10	13
Spacecraft oscillator drift	0.2	0.01	1
Instrumentation	3.3	0.12	15
Baseline	0.2	0.01	1
RSS total	8.0	0.29	36

Table 2. Spacecraft orbital elements referred to the Martian equator of date.

Element	Mars Observer	Mars '94
Semimajor axis, km	3749.288	12650.0
Eccentricity	0.00382	0.7
Inclination, deg	92.821	105.0
Argument of perigee, deg	−90.0	−90.0
Longitude of ascending node, deg	322.773	0.0
Mean anomaly, deg	0.0	0.0
Period, hr	1.94	12.0
Epoch	June 1, 1995, 19:50 UTC	June 1, 1995, 19:50 UTC

Table 3. Assumptions for orbit determination covariance analysis.

Adjusted parameters	A priori sigma
Spacecraft epoch state position	10^4 km per component
Spacecraft epoch state velocity	10 km/sec per component
Unadjusted parameters	**A priori sigma**
Solar reflection coefficients	10 percent of nominal value
Atmospheric drag coefficient	20 percent of nominal value
Bias acceleration	10^{-12} km/sec^2 per component
Mars GM[a]	3.5×10^{-6} × nominal GM
Mars gravity field (spherical harmonics and mascons)	Errors from MO calibration orbit
Station locations (including UT1–UTC and polar motion)	7 cm per component
Zenith troposphere	4 cm
Line-of-sight ionosphere	3 cm

[a] GM = (Mass of Mars) + Newton's gravitational constant

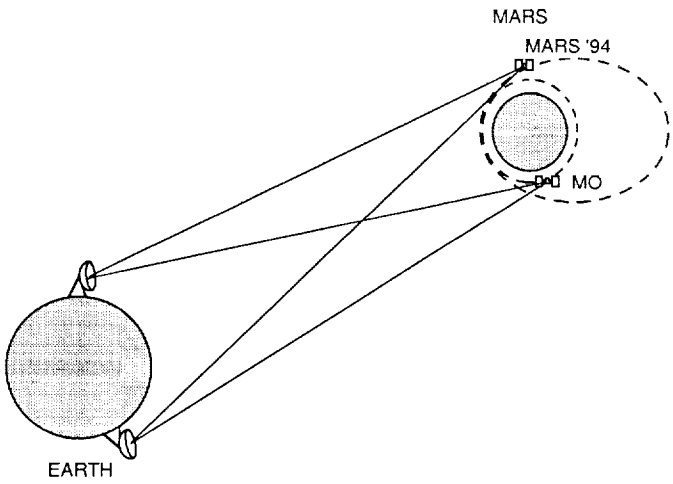

Fig. 1. Same-beam interferometry technique.

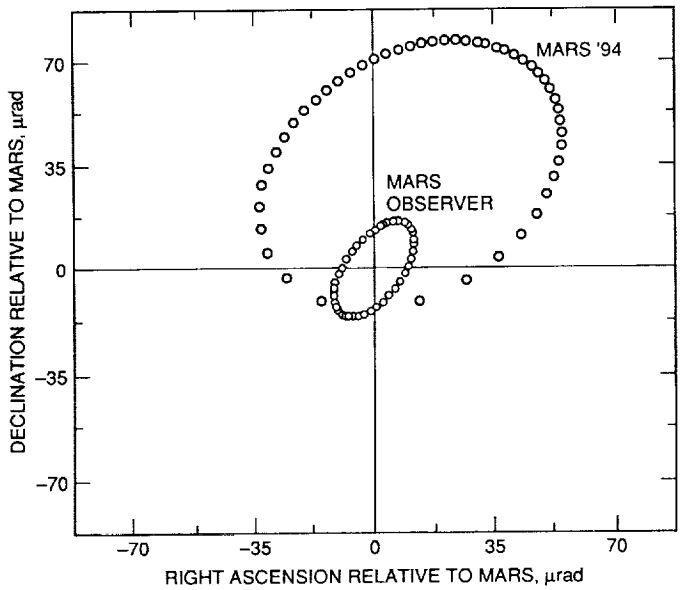

Fig. 3. MO and Mars '94 orbits centered about Mars as seen from Earth on 1-June-1995.

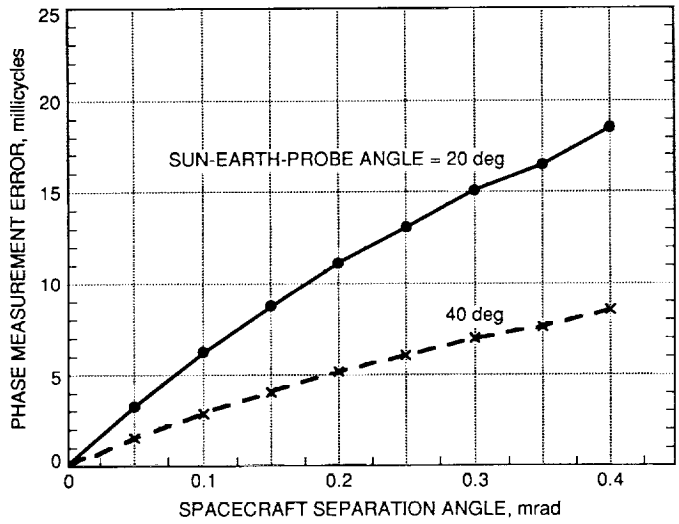

Fig. 2. Effect of solar plasma on X-band same-beam interferometry data for various spacecraft separation angles and Sun-Earth-Probe angles as calculated from model of Kahn (Ref. 5).

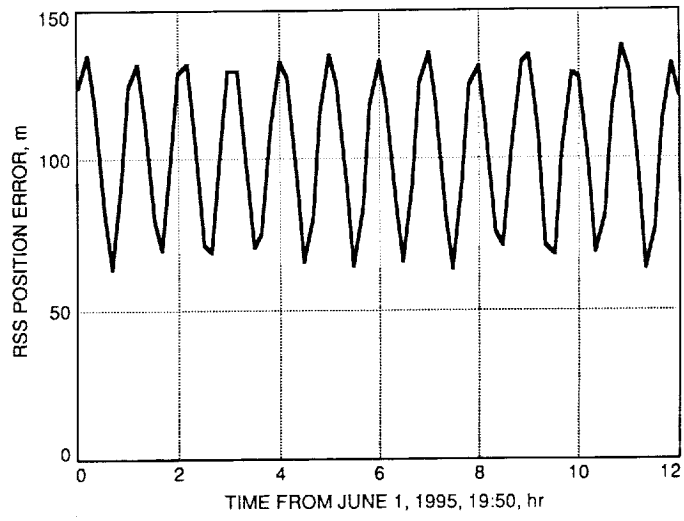

Fig. 4. Doppler-only orbit determination accuracy for Mars Observer.

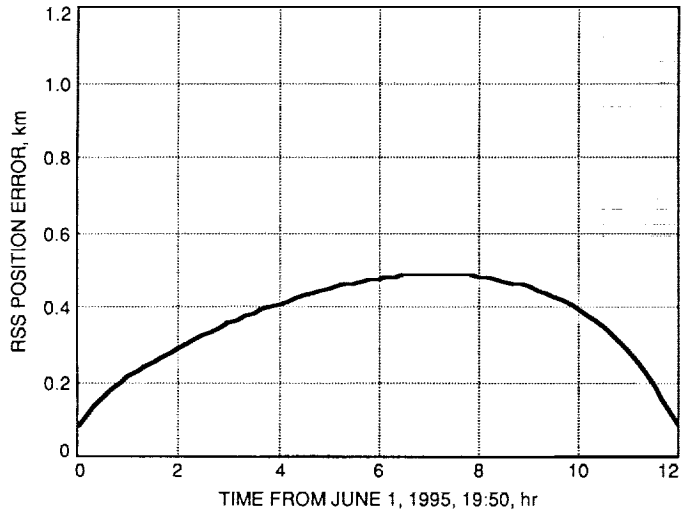

Fig. 5. Doppler-only orbit determination accuracy for Mars '94.

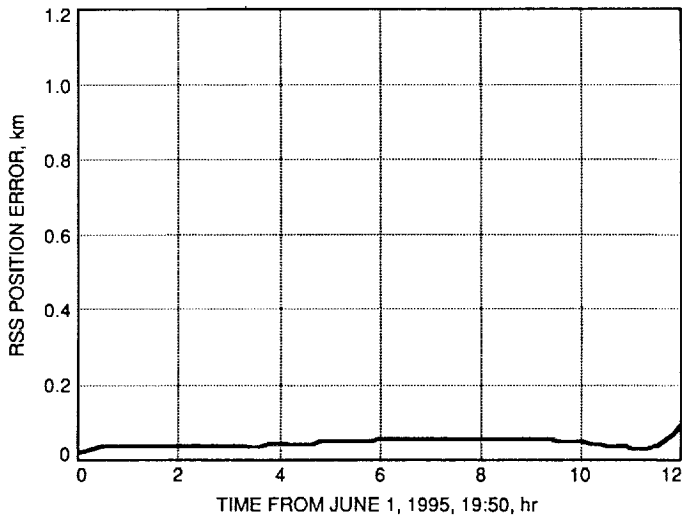

Fig. 7. Doppler plus SBI orbit determination accuracy for Mars '94.

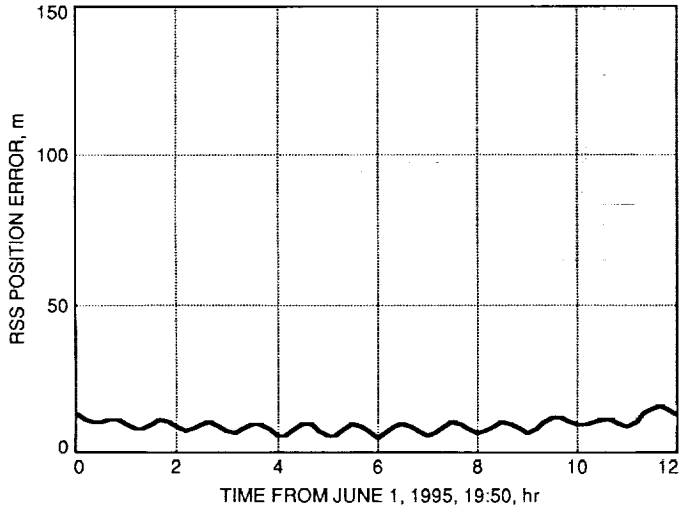

Fig. 6. Doppler plus SBI orbit determination accuracy for Mars Observer.

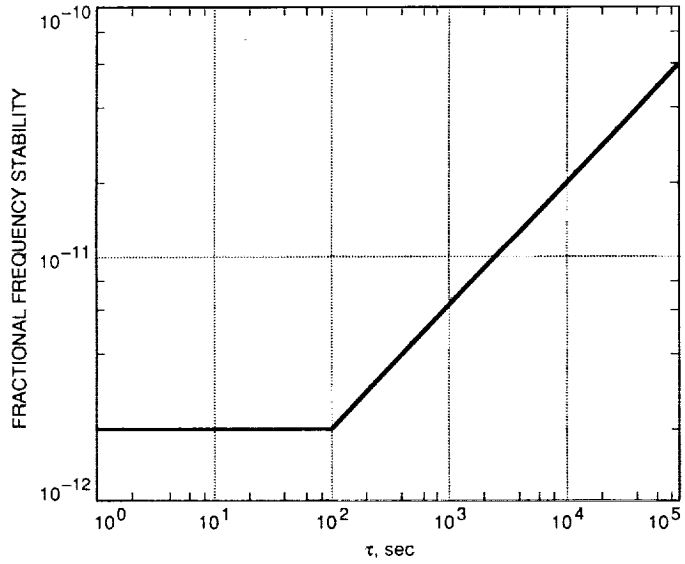

Fig. 8. Assumed stability for Mars '94 oscillator.

C-2

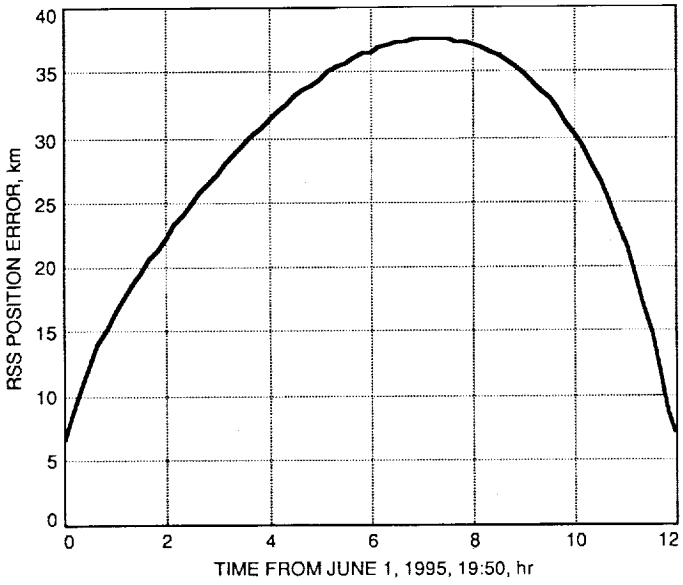

Fig. 9. One-way Doppler orbit determination accuracy for Mars '94.

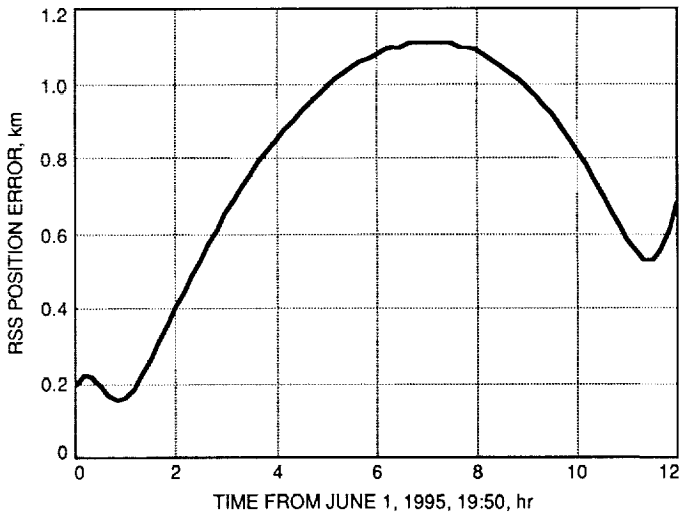

Fig. 11. Orbit determination accuracy for Mars '94 with one-way Doppler combined with bias-estimated SBI and two-way Doppler from Mars Observer.

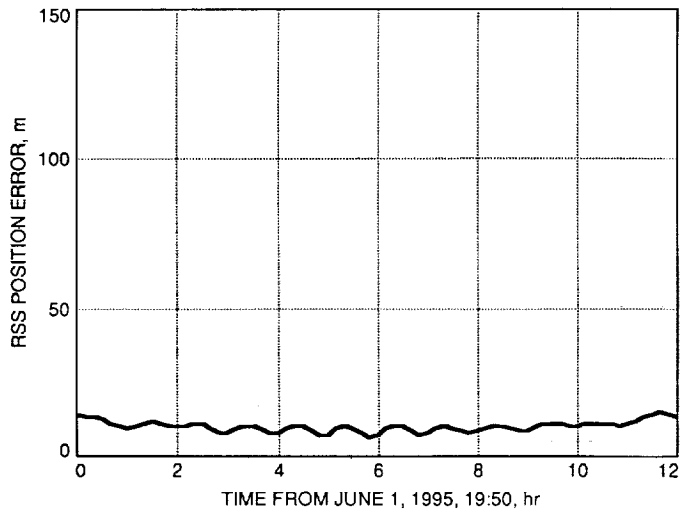

Fig. 10. Orbit determination accuracy for Mars Observer with two-way Doppler combined with bias-estimated SBI and one-way Doppler from Mars '94.

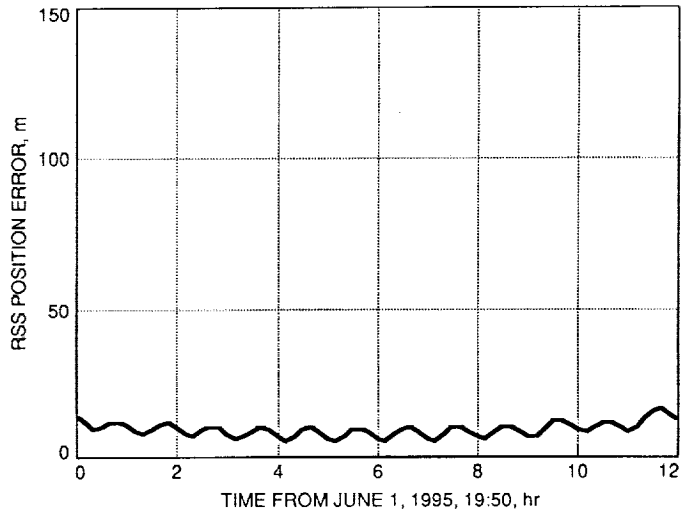

Fig. 12. Orbit determination accuracy for Mars Observer with two-way Doppler combined with bias-fixed SBI and one-way Doppler from Mars '94.

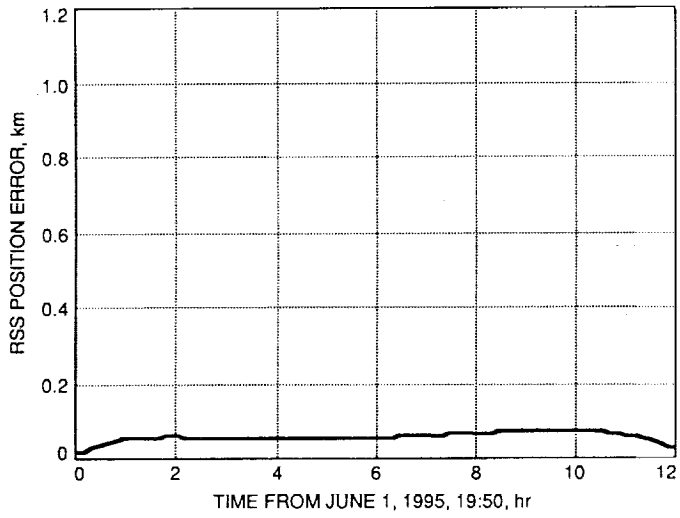

Fig. 13. Orbit determination accuracy for Mars '94 with one-way Doppler combined with bias-fixed SBI and two-way Doppler from Mars Observer.

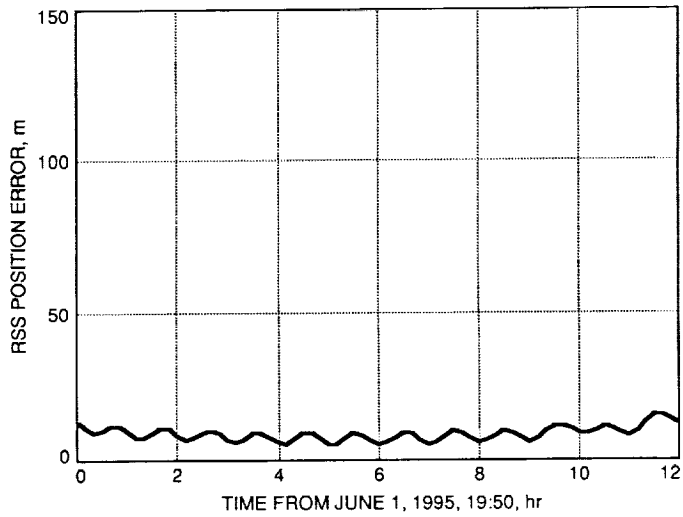

Fig. 14. Orbit determination accuracy for Mars Observer with two-way Doppler combined with SBI and two-way Doppler for the lander.

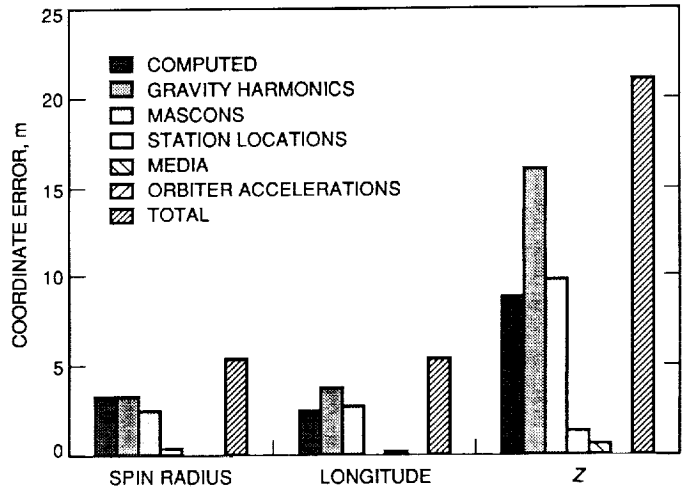

Fig. 15. Mars lander position determination using Doppler and SBI tracking with respect to an orbiter.